**OPEN ACCESS**

Correspondence: T. T. Ashezua

Email: [timothy.ashezua@uam.edu.ng](mailto:timothy.ashezua@uam.edu.ng)

*Specialty Section; This article was submitted to Sciences a section of NAPAS.*

Submitted: 23/02/2024

Accepted: 15/05/2024

Published:

**Citation:**

E. P. Allu, T. Aboiyar, and T. T. Ashezua (2024). Mathematical Analysis of An Avian Influenza Model 7(1):77-91

DOI: [10.5281/zenodo.7338397](https://doi.org/10.5281/zenodo.7338397)

Publisher: cPrint, Nig. Ltd

Email: [cprintpublisher@gmail.com](mailto:cprintpublisher@gmail.com)

## Mathematical Analysis of An Avian Influenza Model

Allu E. P.<sup>1</sup>, Aboiyar T.<sup>2</sup> and Ashezua T. T.<sup>3</sup>

<sup>1,2,3</sup> Department of Mathematics, Joseph Sarwuan Tarka University, Makurdi

**Abstract**

In this paper, a mathematical model for the transmission dynamics of an Avian Influenza is developed and analyzed. The model incorporates vaccination and public enlightenment campaign in the human population. The effective reproduction number is computed using the next generation method. Further, the disease-free equilibrium is shown to be locally and globally asymptotically stable whenever the associated reproduction number is less than unity. Sensitivity analysis results show that some of the most sensitive parameters are the infection transmission rate for the bird ( $\alpha_A$ ), isolation rate of human with avian strain ( $\epsilon_H$ ) and public enlightenment campaign ( $\theta_H$ ). Results from the numerical simulation indicate that vaccination and public enlightenment should be strengthened in order to curtail the spread of the disease in the population.

**Key words:** Avian influenza, Effective reproduction number, Mathematical model, Numerical simulation, Sensitivity analysis.

**Introduction**

Avian influenza (AI) is caused by specified viruses that are members of the family *Orthomyxoviridae* and placed in the genus influenza virus A. There are three influenza genera-A, B and C; only influenza A viruses are known to infect birds. Diagnosis is by isolation of the virus or by detection and characterization of fragments of its genome. This is because infections in birds can give rise to a wide variety of clinical signs that may vary according to the host, strain of virus, the host's immune status, presence of any secondary exacerbating organisms and environmental conditions (World Health Organization (WHO), 2023).

Globally, about 878 cases of human infection with avian influenza A (H5NI) were reported from 23 countries between January 2003 to 14<sup>th</sup> July, 2023 of these 878 cases, 458 were noted to be fatal (WHO, 2023). In Nigeria it was reported that between 2021 and 2022, HPAI caused about 467 outbreaks (Meseko *et al.* 2023)

Avian influenza viruses can be transmitted directly from wild birds to domestic poultry or indirectly e.g., through contaminated materials. The virus spreads directly from bird to bird via airborne transmission

or indirectly, through faecal contamination of material, feathers or feed (Center for Disease Prevention and Control (CDC), 2022).

Infected birds can spread the virus through saliva, nasal secretions, and droppings. Healthy birds get infected when they come into contact with contaminated secretions or feces from infected birds. Contact with contaminated surfaces such as cages might also allow the virus to transfer from bird to bird. Contact with humans occurs in the same way, mainly by flocks of poultry cultivated by farmers that are exposed to wild birds infected with bird flu. Other people are exposed to the bird flu when, for example, infected birds are processed for sale before they are cooked or if they come in contact with contaminated wild bird droppings or dead birds. (CDC, 2022). Humans may get bird flu from contact with infected birds such as turkeys, geese and domestic chicken. The virus can be shed in the droppings of migratory birds since they are natural carriers and is able to survive for three months in cool temperature. It can also survive in water at  $0^{\circ}\text{C}$  for more than 30 days and at  $22^{\circ}\text{C}$  for up to four days. Human-to-human spread of bird flu may occur but has been very rare so far. However, if the highly pathogenic strains of bird flu (H5N1, H7N9) mutate to allow them to be easily transmitted from human to human, investigators are concerned that a lethal pandemic could occur in humans. The incubation period for avian influenza is 2 to 5 days on average and up to 17 days. (CDC, 2022).

Symptoms of the condition in birds depend on the pathogenicity of the virus that infects a bird. A virus that is not highly pathogenic causes mild illness. This form of the condition produces ruffled feathers or a decrease in egg production in infected birds. The highly pathogenic form of the virus can kill so quickly that once the virus enters the birds, the bird may die the same day. In human, avian influenza causes symptoms similar to the typical flu such as aching muscles, cough, fever, sore throat and eye irritation. The symptoms usually appear within 1 to 5 days after contact with the virus. The condition may be life-threatening because of the complication that can occur. These include viral pneumonia and extreme difficulty in breathing. (WHO, 2023).

Mathematical models of infectious diseases

have over the years, provided useful insight into the transmission dynamics and control of infectious diseases (Gumel *et al.* 2017). A number of mathematical models have been developed and analyzed to help understand the transmission dynamics of avian influenza. For example,

Mishra and Sinha (2016) developed a mathematical model on avian influenza with quarantine and vaccination. Their model was subdivided into human and bird population. The basic reproduction number for both epidemic models was computed which showed that their model was found to be locally and globally asymptotically stable for disease free equilibrium point. Also, extensive numerical simulations and sensitivity analysis for various parameters of the model were carried out. The result shows clear evidence that quarantine and vaccination play vital role for early recovery of the disease.

Further Chairat (2017) designed a mathematical model of an avian influenza and optimal control theory for intervention strategies. The optimal control is to seek cost effectiveness for control and treatment strategies. Their result shows that strategically deployed vaccination and medical treatment can significantly reduce the numbers of exposed and infectious persons in the population. Kharis and Amidi (2018) formulated a mathematical model and then analyzed it to determine the equilibrium points and their stability. Mouaouine *et al.* (2018) formulated a model that discussed the stability of the SIR epidemic based on the basic reproduction number at two equilibrium points (disease-free and endemic). Xiangjun *et al.* (2020) presents a mathematical model to understand the transmission dynamics of avian influenza A(H7N9) in China. The model incorporates various factors such as poultry-to-human and human-to-human transmission, and provides insights into the impact of control measures. Hertz (2022) developed a model that focuses on understanding and predicting the mutation rates of avian influenza viruses. Avian influenza viruses pose a significant threat to both avian and human populations, as they have the potential to cause deadly pandemics. Kang *et al.* (2019) designed a model on avian influenza and its transmission to virus compartment and showed how to control and minimize the outbreak from birds to human. Kimbir *et al.*, (2014) an extension

of the model proposed by Okosun and Yusuf (2007) formulated a model by incorporating the culling of infected birds and isolation of infected humans with Avian Influenza. In describing the model, the total avian (birds) population was subdivided into susceptible wild birds, susceptible domestic birds, infected wild birds, and infected domestic birds while in the human population, the assumption was that humans infected with avian influenza cannot infect susceptible humans. Thus, a subdivision of the total human population into susceptible humans, infected humans, isolated infected humans, and recovered humans. The study allowed for the recovery of infected humans. The model showed that the biological feasible region was positively – invariant and attracting and a numerical simulation showed that any control strategy aimed at reducing the infection transmission will positively influence the eradication of Avian Influenza infection.

In all the aforementioned works, none has incorporated public enlightenment campaign and vaccination in the human population. Thus, in this work a mathematical model for avian influenza is developed incorporating public enlightenment campaign and vaccination in the human population.

**Model Formulation**

The total population at time t, denoted by  $N(t)$ , is divided into the human population ( $N_H(t)$ ), and bird population ( $N_B(t)$ ). The total human population is further subdivided into the susceptible humans ( $S_H(t)$ ), infected humans ( $I_H(t)$ ), isolated humans ( $Q_H(t)$ ), vaccinated humans ( $V_H(t)$ ) and recovered humans ( $R_H(t)$ ). Also, the bird population is subdivided into susceptible wild bird ( $S_W(t)$ ), susceptible domestic birds ( $S_D(t)$ ), infected wild birds ( $I_W(t)$ ), and infected domestic birds ( $I_D(t)$ ). Thus,

$$\begin{aligned}
 N(t) &= N_H(t) + N_B(t) \\
 N_H(t) &= S_H(t) + I_H(t) + Q_H(t) + V_H(t) + R_H(t) \\
 N_B(t) &= S_W(t) + S_D(t) + I_W(t) + I_D(t)
 \end{aligned}
 \tag{1}$$

The susceptible population (for both human and domestic birds) are increased by the recruitment of human and domestic (wilds) birds into the population at the rate  $\beta_H$  and  $\beta_D(\beta_W)$ , respectively. The susceptible humans acquire the infections

following effective contact with infected humans at a rate  $\lambda_H$  while both the susceptible domestic and wilds birds acquire the infection at the rate  $\lambda_D$  and  $\lambda_W$ , respectively.

The parameters  $\alpha_W$ ,  $\alpha_D$  and  $\alpha_A$  represents the infection transmission rates for birds, respectively.

Individuals in  $I_H$  progress to  $Q_H$  at a rate  $\epsilon$  individuals in  $Q_H$  can recover and move to class  $R_H$  due to natural immunity at a rate,  $\tau$ . Also, susceptible human can be vaccinated and move to  $V_H$  at a rate  $\gamma$ . However, the vaccine wanes at a rate  $\phi$  The individuals in  $R_H$  can loose immunity and move to class  $S_H$  at a rate,  $\sigma$ . The parameters  $\theta_H$  and  $\psi$  stands for public enlightenment campaign and its efficacy, respectively. Furthermore, the parameters for natural death rate,  $\mu$  is associated to all the epidemiological classes, while individuals in  $I_H$  and domestic (wild) birds in  $I_D(I_W)$  classes suffered additional death burden at  $\delta_H$  and  $\delta_D(\delta_W)$ , respectively. From the above definitions and assumption, it follows that the model for modelling the transmission dynamics of avian influenza incorporating public enlightenment campaign as control measures is given by the following system of differential equations (a schematic diagram of the model is presented in figure 1, and the variables and parameters of the model are tabulated in table 1):

**Table 1: Variables and parameters of the Model (2)**

Parameters	Definitions
$N_w(t)$	Total number of wild birds at time t
$N_D(t)$	Total number of domestic birds at time t
$N_H(t)$	Total number of humans at time t
$S_w(t)$	Total number of susceptible wild birds at time t
$I_w(t)$	Total number of infected wild birds at time t
$S_D(t)$	Total number of susceptible domestic birds at time t
$I_D(t)$	Total number of infected domestic birds at time t
$S_H(t)$	Total number of susceptible humans at time t
$I_H(t)$	Total number of infected humans at time t
$Q_H(t)$	Total number of isolated humans with avian strain at time t
$R_H(t)$	Total number of recovered humans at time t
$\beta_w$	Average birth rate in wild birds
$\beta_D$	Average birth rate in domestic birds
$\alpha_w \alpha_D \alpha_A$	Infection transmission rates for birds
$\eta$	Destruction (culling) rate for infected birds
$\mu_B$	Natural death rate in birds
$\delta_w$	Flu induced death rate in wild birds
$\delta_D$	Flu induced death rate in domestic birds
$\beta_H$	Average birth rate in humans
$\mu_H$	Natural death rate in humans
$\delta_H$	Flu induced death rate in humans
$\epsilon_H$	Isolation rate of humans with avian strain
$\vartheta_H$	Flu induced death rate in isolated humans ( $\vartheta_H \propto d_H$ )
$\omega$	Recovery rate without immunity
$\gamma$	Recovery rate with substantial immunity
$V_H(t)$	Total number of vaccinated humans at time t
$\theta_H$	Public enlightenment campaign
$\gamma_H$	Rate at which susceptible humans are vaccinated
$\phi_H$	Loss of vaccine-induced immunity
$\tau_H$	Recovery rate due to natural immunity
$\psi$	Efficacy of public enlightenment campaign

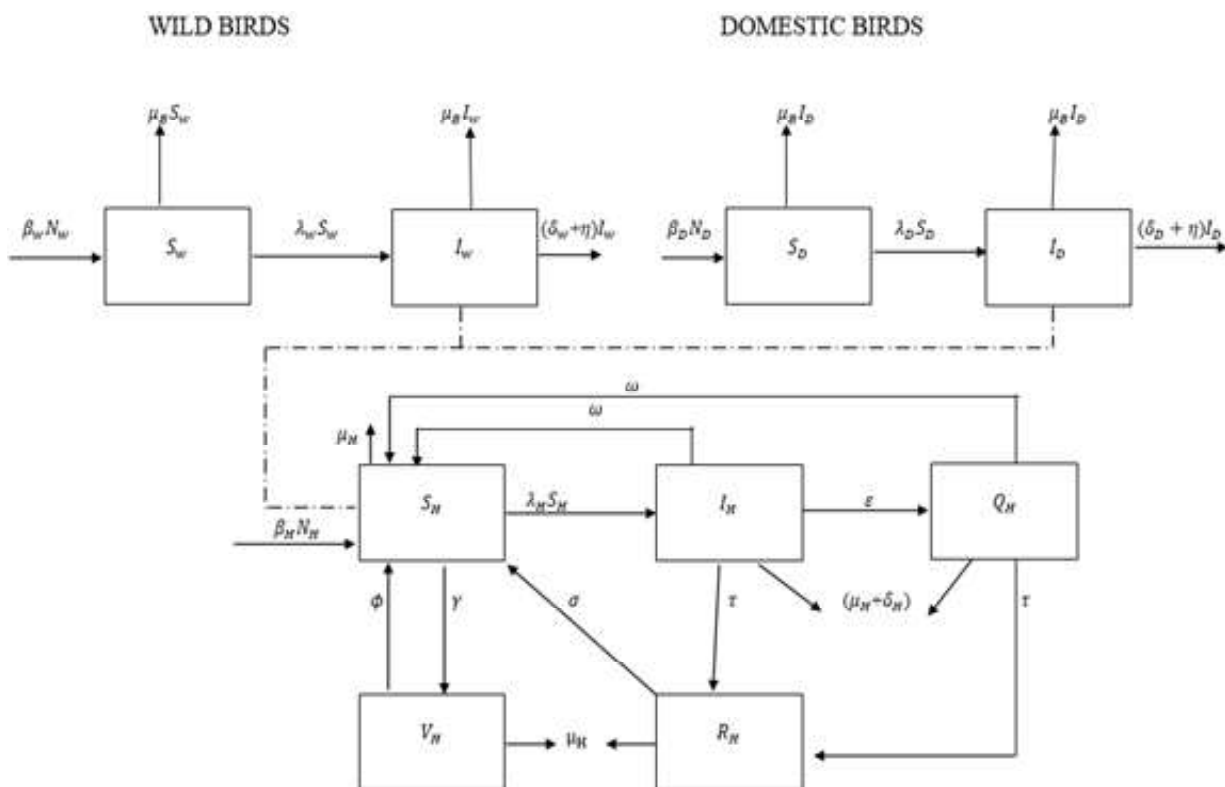


**Figure 1:** Schematic diagram for model (2)  
From the schematic diagram in Figure 1, we obtain the following set of differential equations

$$\left. \begin{aligned} \frac{dS_H}{dt} &= \beta_H N_H + \omega I_H + \omega Q_H + \phi V_H + \sigma R_H - \lambda_H S_H - (\mu_H + \gamma) S_H \\ \frac{dI_H}{dt} &= \lambda_H S_H - (\mu_H + \omega + \varepsilon + \tau) I_H \\ \frac{dQ_H}{dt} &= \varepsilon I_H - (\mu_H + \delta_H + \omega + \tau) Q_H \\ \frac{dV_H}{dt} &= \gamma S_H + (\mu_H + \phi) V_H \\ \frac{dR_H}{dt} &= \tau I_H + \tau Q_H - (\mu_H + \sigma) R_H \\ \frac{dS_W}{dt} &= \beta_W N_W - \lambda_W S_W - \mu_B S_W \\ \frac{dI_W}{dt} &= \lambda_W S_W - (\mu_B + \delta_W + \eta) I_W \\ \frac{dS_D}{dt} &= \beta_D S_D - \lambda_D S_D - \mu_B S_D \\ \frac{dI_D}{dt} &= \lambda_D S_D - (\mu_B + \delta_D + \eta) I_D \end{aligned} \right\} (2)$$

The model (2) complements other models for avian influenza transmission dynamics in the literature (such as the one by Kimbir *et al.* 2014) by:

- i. Incorporating public enlightenment campaign and its efficacy in the human population.
- ii. Introduced a vaccinated class for the human population.

We proved theorem 2.1 below following the approach as outlined in the works Gumel *et al.* (2017).

**Theorem 2.1:** All solutions of the model system (2) with positive initial data remain positive for all time  $t > 0$ . Furthermore, the model is a dynamical system on the region

$$\Omega = \Omega_H \cup \Omega_B \subset R_+^5 \times R_+^4$$

With

$$\Omega_H = \left\{ (v_H, S_H, i_H, q_H, r_H) : \begin{aligned} v_H + S_H + i_H + \\ q_H + r_H = n_H \leq 1 \end{aligned} \right\}$$

$$\Omega_B = \{ (S_W, S_D, i_W, i_D, ) : S_W + S_D + i_W + i_D \leq 1 \}$$

and the region  $\Omega$  is attracting with respect to the model (2) with the initial conditions in  $R_+^9$ .

**Proof:** It can be verified that the equations for the human and birds' susceptible population in the

model (2) leads to the following first-order inequality equations.

$$\begin{aligned} \frac{dS_H}{dt} + (\lambda_H + \mu_H + \gamma) S_H &> 0 \\ \frac{dS_W}{dt} + (\lambda_W + \mu_B) S_W &> 0 \text{ and} \\ \frac{dS_D}{dt} + (\lambda_D + \mu_B) S_D &> 0 \end{aligned}$$

Multiplying the above inequalities by the integrating factors

$$\alpha_H(t) = \exp\left(\int_0^t (\lambda_H + \mu_H + \gamma) ds\right)$$

$$\alpha_W(t) = \exp\left(\int_0^t (\lambda_W + \mu_B) S_W\right)$$

and

$$\alpha_D(t) = \exp\left(\int_0^t (\lambda_D + \mu_B) S_D\right)$$

and carefully observed that

$$\alpha_H \left[ \frac{dS_H}{dt} + (\lambda_H + \mu_H + \gamma) S_H \right] = \frac{d(S_H \alpha_H)}{dt}$$

$$\alpha_W \left[ \frac{dS_W}{dt} + (\lambda_W + \mu_B) S_W \right] = \frac{d(S_W \alpha_W)}{dt}$$

and

$$\alpha_D \left[ \frac{dS_D}{dt} + (\lambda_D + \mu_B) S_D \right] = \frac{d(S_D \alpha_D)}{dt}$$

then integration with respect to time from 0 to  $t$  gives  $S_H \geq 0$ ,  $S_W \geq 0$  and  $S_D \geq 0$  at all times, respectively. This approach does not however apply to the rest of the equations. This is because at disease-free equilibrium, the rest of the equations involving the infected compartments will vanish.

Furthermore, noting the non-negativity of  $S_H$ ,  $S_W$  and  $S_D$  in mind it can be shown that the rest of the equations in model (2) form a monotone system.

Hence, all its solution corresponding to positive initial data remain positive at all times  $t \geq 0$  (Smith, 1995). Summing the first five and the last four equation of the model (2) leads to the conservation law.

$$\frac{dn_H(t)}{dt} \leq \beta_H - \beta_H n_H$$

$$\frac{dn_B(t)}{dt} \leq \beta_B - \beta_B n_B$$

Thus, a standard comparison theorem or Gronwall inequality can be used to show that the general a priori estimates below hold.

$$0 \leq n_H(t) \leq 1 + (n_H(0) - 1)e^{-\beta_H t}$$

$$0 \leq n_B(t) \leq 1 + (n_B(0) - 1)e^{-\beta_B t}$$

In particular, we have a priori estimated

$$0 \leq n_H(t) \leq 1 \text{ if } n_H(0) \leq 1$$

$$0 \leq n_B(t) \leq 1 \text{ if } n_B(0) \leq 1$$

Combining these a priori estimates, we conclude that there exists a unique global solution in the domain  $\Omega$ . Thus, the model (2) is dynamical system on  $\Omega$ . On the other hand, if a solution is outside the region  $\Omega$ , that is  $n_H(t) \geq 1$  and  $n_B(t) \geq 1$  then, it follows from the above conservation law that  $\frac{dn_H}{dt} \leq 0$  and  $\frac{dn_B}{dt} \leq 0$ . Hence, the above general estimates show that  $n_H(t)$  and  $n_B(t)$  tends to 1 as  $t \rightarrow \infty$ . Thus, the region  $\Omega$  is attracting.

**METHODS**

**Model Equations in Proportion**

We defined the proportion for each class as follows;

$$\left. \begin{aligned} \frac{ds_H}{dt} &= \beta_H + \Phi v_H + \sigma r_H + \omega(i_H + q_H) - \lambda_H s_H - (\beta_H + \gamma) s_H + \delta_H i_H s_H + \delta_H q_H s_H \\ \frac{di_H}{dt} &= \lambda_H s_H - (\beta_H + \delta_H + \omega + \varepsilon + \tau) i_H + \delta_H q_H i_H + \delta_H i_H^2 \\ \frac{dq_H}{dt} &= \varepsilon i_H - (\beta_H + \delta_H + \omega + \tau) q_H + \delta_H i_H q_H + \delta_H q_H^2 \\ \frac{dv_H}{dt} &= \gamma s_H + (\beta_H + \Phi) v_H + \delta_H i_H v_H + \delta_H q_H v_H \\ \frac{dr_H}{dt} &= \tau(i_H + q_H) - (\beta_H + \sigma) r_H + \delta_H i_H r_H + \delta_H q_H r_H \\ \frac{ds_W}{dt} &= \beta_W - \beta_W s_W - \lambda_W s_W + (\delta_w + \eta) i_B s_W \\ \frac{di_W}{dt} &= \lambda_W s_W - (\beta_w + \delta_W + \eta) i_W + (\delta_w + \eta) i_W^2 \\ \frac{ds_D}{dt} &= \beta_D - \beta_D s_D - \lambda_D s_D + (\delta_D + \eta) i_B s_D v \\ \frac{di_D}{dt} &= \lambda_D s_D - (\beta_D + \delta_D + \eta) i_D + (\delta_D + \eta) i_D^2 \end{aligned} \right\} \tag{3}$$

where,

$$\left. \begin{aligned} \lambda_B &= (1 - \theta_H \psi)(\alpha_B i_w + \alpha_B i_D + \alpha_A i_H) \\ \lambda_w &= \alpha_w (i_w + i_D) \\ \lambda_D &= \alpha_D (i_w + i_D) \end{aligned} \right\} \tag{4}$$

The system (3) can be reduced further by setting

$$\left. \begin{aligned} s_w + i_w &= 1, s_w = 1 - i_w \\ s_D + i_D &= 1, s_D = 1 - i_D \\ s_H + i_H + q_H + v_H + r_H &= 1, s_H = 1 - i_H - q_H - v_H - r_H \end{aligned} \right\} \tag{5}$$

$$\left. \begin{aligned}
 \frac{di_H}{dt} &= (1 - \theta_H \psi)(\alpha_B i_w + \alpha_B i_D + \alpha_B i_H)(1 - i_H - q_H - v_H - r_H) \\
 &\quad - (\beta_H + \delta_H + \omega + \varepsilon + \tau)i_H + \delta_H q_H i_H + \delta_H i_H^2 \\
 \frac{dq_H}{dt} &= \varepsilon i_H - (\beta_H + \delta_H + \omega + \tau)q_H + \delta_H i_H q_H + \delta_H q_H^2 \\
 \frac{dv_H}{dt} &= \gamma s_H - (\beta_H + \phi)v_H + \delta_H i_H v_H + \delta_H q_H v_H \\
 \frac{dr_H}{dt} &= \tau(i_H + q_H) - (\beta_H + \sigma)r_H + \delta_H i_H r_H + \delta_H q_H r_H \\
 \frac{di_w}{dt} &= \alpha_w(i_w + i_D)(1 - i_w) - (\beta_w + \delta_w + \eta)i_w - (\delta_w + \eta)i_w^2 \\
 \frac{di_D}{dt} &= \alpha_D(i_w + i_D)(1 - i_D) - (\beta_D + \delta_D + \eta)i_D - (\delta_D + \eta)i_D^2
 \end{aligned} \right\} \quad (6)$$

Redefining (6) we now have

$$\left. \begin{aligned}
 \frac{di_H}{dt} &= \lambda b h(1 - i_H - q_H - v_H - r_H) - \psi_5 i_H + \delta_H q_H i_H + \delta_H i_H^2 \\
 \frac{dq_H}{dt} &= \varepsilon i_H - \psi_6 q_H + \delta_H i_H q_H + \delta_H q_H^2 \\
 \frac{dv_H}{dt} &= \gamma(1 - i_H - q_H - v_H - r_H) - \psi_7 v_H + \delta_H i_H v_H + \delta_H q_H v_H \\
 \frac{dr_H}{dt} &= \tau(i_H + q_H) - \psi_8 r_H + \delta_H i_H r_H + i_H q_H r_H \\
 \frac{di_w}{dt} &= \lambda_w(1 - i_w) - \psi_1 i_w - \psi_2 i_w^2 \\
 \frac{di_D}{dt} &= \lambda_D(1 - i_D) - \psi_3 i_D - \psi_4 i_D^2
 \end{aligned} \right\} \quad (7)$$

The non- negative initial conditions for the model are  $S_W(0) > 0, I_W(0) \geq 0, S_D(0) \geq 0, I_D(0) \geq 0, S_H(0) \geq 0, I_H(0) \geq 0, Q_H(0) \geq 0, R_H(0) \geq 0, V_H(0) \geq 0$

#### Asymptotic stability of disease-free equilibrium (DFE)

The disease-free equilibrium (DFE) of the model (2) is given by

$$\begin{aligned}
 E_0 &= (s_w^0, i_w^0, s_D^0, i_D^0, s_w^0, i_H^0, q_H^0, v_H^0, r_H^0) \\
 &= \left(1, 0, 1, 0, \frac{\beta_H + \phi}{\beta_H + \phi + \gamma}, 0, 0, \frac{\gamma}{\beta_H + \phi + \gamma}, 0\right)
 \end{aligned}$$

The local stability of  $E_0$  will be explored using the next generation operator method ( van dan Driessche and Watmough, 2002). Adopting the notation in Van den Driessche and Watmough, 20 and Diekmann *et al.* 1990, the non-negative matrix, F, of new infection terms and the M-matrix, V, of the transition terms associated with the model (2) are

$$F = \begin{pmatrix} \alpha_w & \alpha_w & 0 \\ \alpha_D & \alpha_D & 0 \\ a_1 & a_2 & a_3 \end{pmatrix}$$

and

$$V = \begin{pmatrix} \psi_1 & 0 & 0 \\ 0 & \psi_3 & 0 \\ 0 & 0 & \psi_5 \end{pmatrix}$$

where,

$$a_1 = (1 - \theta)\alpha_B(1 - v_H^0)$$

$$a_2 = (1 - \theta)\alpha_B(1 - v_H^0)$$

$$a_3 = (1 - \theta)\alpha_A(1 - v_H^0)$$

It follows that the effective reproduction number of the model (2), denoted by  $R_eH = \rho(FV^{-1})$  (where  $\rho$  denotes the spectral radius), is given by

$$R_eH = \frac{\alpha_A(1-\theta_H)(\beta_H+\phi)}{(\beta_H+\phi+\gamma)(\beta_H+\delta_H+\omega+\varepsilon+\tau)} \quad (8)$$

The result below follows from Theorem 2 in van den Driessche and Watmough, (2002).

**Lemma 3.1:** The DFE of the model (2), given by  $E_0$ , is locally asymptotically stable if  $R_eH < 1$  and unstable if  $R_eH > 1$ .

The threshold quantity  $R_eH$  measures the average number of new avian influenza infections generated by a single infected bird/ human in a completely susceptible population (Van den Driessche and Watmough, (2002). Lemma 3.1 implies that avian influenza can be effectively controlled in the population if the initial sizes of the subpopulations of the model are in the basin of attraction of the DFE ( $E_0$ ). To ensure that disease eradication is independent of the initial sizes of the subpopulations, it is necessary to show that the DFE is globally asymptotically stable if  $R_eH < 1$ . This is considered in the next section.

### Global Stability of the Disease-free Equilibrium

**Theorem 4:** If  $R_e < 1$ , the disease-free equilibrium point is globally asymptotically stable and unstable if  $R_e > 1$ .

#### Proof:

By the comparison theorem, the rate of change of the variables representing the infected compartments of the system (2) can be rewritten as

$$\begin{pmatrix} \frac{di_w}{dt} \\ \frac{di_D}{dt} \\ \frac{di_H}{dt} \end{pmatrix} = (F - V) \begin{pmatrix} i_w \\ i_D \\ i_H \end{pmatrix} = \begin{pmatrix} \alpha_w(i_w + i_D) \\ \alpha_D(i_w + i_D) \\ \varphi_9 \end{pmatrix} \quad (9)$$

where,

$$\varphi_9 = (1 - \theta)(\alpha_B i_w + \alpha_B i_D + \alpha_A i_H)$$

$$(1 - i_H - q_H - v_H - \gamma_H)$$

also

$$F = \begin{pmatrix} \alpha_w & \alpha_w & 0 \\ \alpha_D & \alpha_D & 0 \\ \frac{\alpha_B(1-\theta)(\beta_H+\phi)}{\beta_H+\phi+\gamma} & \frac{\alpha_B(1-\theta)(\beta_H+\phi)}{\beta_H+\phi+\gamma} & \frac{\alpha_A(1-\theta)(\beta_H+\phi)}{\beta_H+\phi+\gamma} \end{pmatrix}$$

and

$$V = \begin{pmatrix} \varphi_1 & 0 & 0 \\ 0 & \varphi_3 & 0 \\ 0 & 0 & \varphi_5 \end{pmatrix}$$

Hence, we obtain,

$$\begin{pmatrix} \frac{di_w}{dt} \\ \frac{di_D}{dt} \\ \frac{di_H}{dt} \end{pmatrix} = \begin{pmatrix} \alpha_w - \varphi_1 & \alpha_w & 0 \\ \alpha_D & \alpha_D - \varphi_3 & 0 \\ \frac{\alpha_B(1-\theta)(\beta_H+\phi)}{\beta_H+\phi+\gamma} & \frac{\alpha_B(1-\theta)(\beta_H+\phi)}{\beta_H+\phi+\gamma} & \frac{\alpha_A(1-\theta)(\beta_H+\phi)}{\beta_H+\phi+\gamma} - \varphi_5 \end{pmatrix} \begin{pmatrix} i_w \\ i_D \\ i_H \end{pmatrix} \quad (10)$$

Furthermore, having all the eigenvalues of matrix  $(F - V)$  with negative real parts, we observed from (10) that the linearized differential inequality is stable whenever  $R_e W, R_e D$  and  $R_e H < 1$  ( $R_e < 1$ ). Consequently,  $(i_w, i_D, i_H) \rightarrow (0,0,0)$  as  $t \rightarrow \infty$ . Therefore,  $s_H^0 = \frac{\beta_H+\phi}{\beta_H+\phi+\gamma}$  and  $v_H^0 = \frac{\gamma}{\beta_H+\phi+\gamma}$  for  $R_e < 1$ . Hence, the disease-free equilibrium point  $\varepsilon_0$  is globally asymptotically stable.

## RESULTS AND DISCUSSION

In this section, sensitivity analysis and numerical simulations are carried out on model (2). The results are presented and discussed.

### Sensitivity Analysis

Here, we conduct sensitivity analysis on the parameters of the model associated with the effective reproduction number,  $R_e$  using the parameter values in Table 2.

The essence of this analysis is to determine the relative importance of each parameter in the model that depicts avian influenza transmission. A method similar to the ones outlined in the works of Anna *et al.* (2020), Rangkuti *et al.* (2022) Ashezua *et al.* (2023) were utilized to obtain the sensitivity index of all the parameters connected to the reproduction number as follows.

**Definition:** (Annal *et al.* 2020). The normalized forward sensitivity index of a variable  $R_e$ , which is differentiable on the parameter  $\beta$  is defined as

$$S_\beta^{R_e} = \frac{\partial R_e}{\partial \beta} \times \frac{\beta}{R_e} \quad (11)$$

Using (11), we obtained the sensitivity indices of the parameters associated with the reproduction number as presented in Table 3.

From Table 3, parameters with positive sensitivity indices signify a high impact burden of avian influenza in the population if their values keep increasing. In a similar manner, parameters in which their sensitivity indices are negative have a great effect in reducing avian influenza burden in the population as their values increase while the others remain constant. Hence, as their values increase, the reproduction number decreases thus minimizing the endemicity of the disease in the population.

From the results of the sensitivity analysis presented in Table 3, observe that some of the parameters are loose of immunity  $\omega_H$ , substantial immunity in humans  $\tau_H$ , death rate in humans  $\delta_H$ , isolation rate of humans  $\varepsilon_H$ , and public enlightenment campaign  $\theta_H$  have high negative index. Consequently, to control the spread of the disease, these top parameters must be effectively targeted by policy makers in the health sector so that the sensitivity indices of these parameters must be kept negative for effective control of the disease.

### Numerical Simulations

In this section, we carryout numerical simulation of the model (2).

This is done by using a set of parameters and initial values of the variables whose sources are mainly from literature, Kimbir et al., (2014) as well as assumed value based on the literature of the disease in order to have more realistic simulation results. Tables 4 and 5 present the values and their respective sources. This implies that the advocacy for the use of control measures by susceptible individuals and proper vaccination of infected individuals must be higher if avian influenza must be curtailed in the population.

**Table 2: Parameter values of Human for Numerical and Sensitivity Analysis**

Parameter	Value	Source
$\alpha_A$	0.3	Kimbir <i>et al.</i> (2014)
$\beta_H$	0.043	Kimbir <i>et al.</i> (2014)
$\delta_H$	0.1	Kimbir <i>et al.</i> (2014)
$\sigma_H$	$4.2 \times 10^{-5}$	Kimbir <i>et al.</i> (2014)
$\vartheta$	$1.7 \times 10$	Kimbir <i>et al.</i> (2014)
$\eta$	0.1	Kimbir <i>et al.</i> (2014)
$\varepsilon_H$	0.3	Kimbir <i>et al.</i> (2014)
$\vartheta_H$	0.05	Kimbir <i>et al.</i> (2014)
$\tau_H$	0.0017	Kimbir <i>et al.</i> (2014)
$\sigma_H$	0.0009	Kimbir <i>et al.</i> (2014)
$\phi_H$	0.02	Mishra <i>et al.</i> (2016)
$\mu_H$	0.000042	Assumed
$\gamma_H$	0.1	Mishra <i>et al.</i> (2016)
$\phi_H$	0.7	Assumed
$\omega_H$	0.0017	Assumed

**Table 3: Initial Values for Variables used in Numerical Simulation**

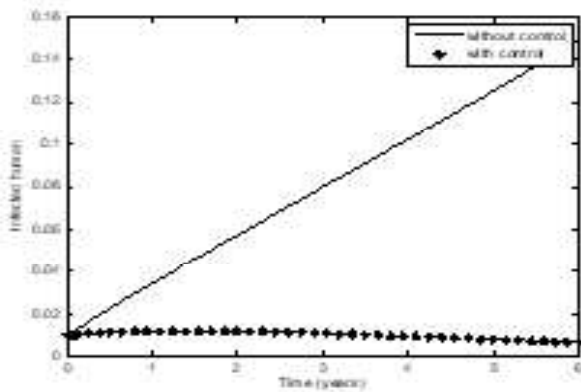
Parameter	Value	Source
$s_w(0)$	0.98	Kimbir <i>et al.</i> (2014)
$i_w(0)$	0.02	Kimbir <i>et al.</i> (2014)
$s_D(0)$	0.98	Kimbir <i>et al.</i> (2014)
$i_D(0)$	0.02	Kimbir <i>et al.</i> (2014)
$s_H(0)$	0.99	Kimbir <i>et al.</i> (2014)
$i_H(0)$	0.01	Kimbir <i>et al.</i> (2014)
$q_H(0)$	0	Kimbir <i>et al.</i> (2014)
$r_H(0)$	0	Kimbir <i>et al.</i> (2014)
$v_H(0)$	0.01	Mishra <i>et al.</i> (2016)

**Table 4: Sensitivity indices of  $R_e$  with respect to each parameter.**

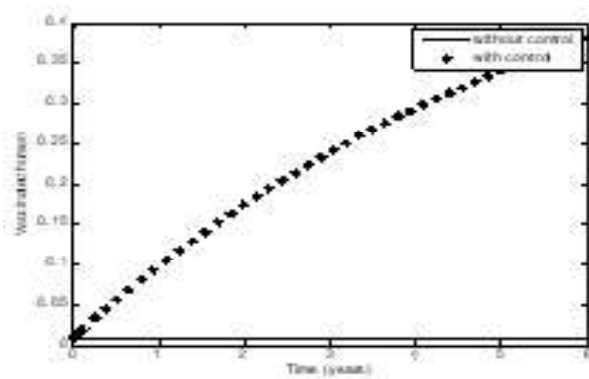
S/N	Parameter	Sensitivity index	Sign
1.	$\alpha_A$	1.0000	+
2.	$\beta_H$	0.3224	+
3.	$\phi_H$	0.1948	+
4.	$\omega_H$	0.0038	-
5.	$\tau_H$	0.0038	-
6.	$\delta_H$	0.2240	-
7.	$\varepsilon_H$	0.6720	-
8.	$\theta_H$	2.3333	-

**Impact of Avian Influenza with or without control on Human Population.**

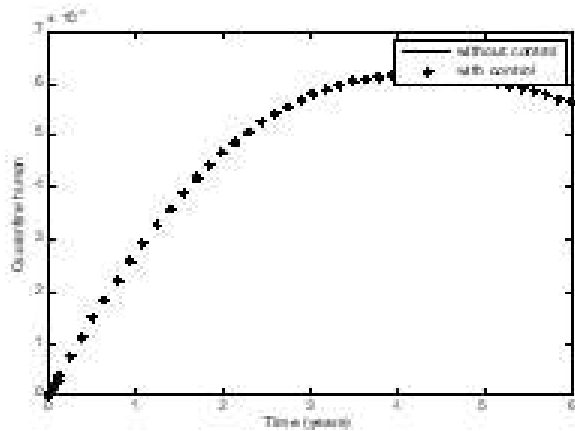
In Figure 3, we show the trends of the avian influenza with or without control in the human population. Figure 3(a) shows that the population without control increases the infected human population but with control measures put in place it shows that it decreases rapidly and therefore the virus gradually will be wiped out of the population after some time. Similarly, it can be easily seen in Figure 3(b) that in the isolated or quarantined human the population of the control is higher because the compartments kept aside for that purpose. It clearly shows that there is no effect of control. Figure 3(c). Indicated that in the vaccinated human, the population in this compartment with control is higher than the one without control. This implies that the population is responding to treatment. In Figure 3(d), it can be observed that the recovered human with control increases than without control, it leads to rapid decrease of the virus in the population, hence the population has recovered from the virus.



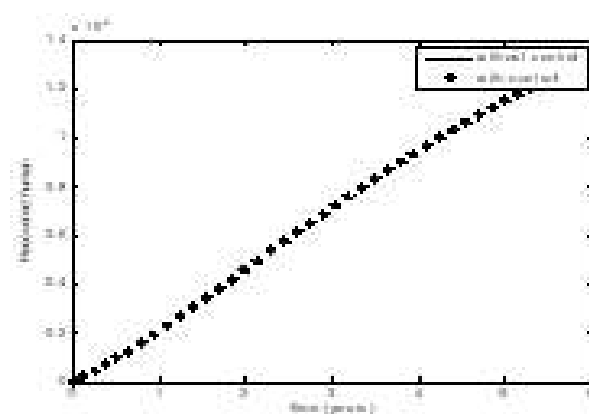
(a)



(c)



(b)



(d)

**Figure 3:** Simulation results showing the trends of the state variable of the avian influenza with without control for (a) Infected Human  $I_H$ , (b) Quarantined Human  $Q_H$  (c) Vaccinated Human and (d) Recovered Human  $R_H$  of the model system

**Impact of Public Health Education Campaign on Infected, Quarantined, Vaccinated and Recovered.**

In Figure 4, we show the role of impact of public health education campaign in the human population.

The number of unaware in the infected population increases fast as shown in Figure 4(a), b when the number of unaware infected population becomes aware of the virus the population decrease rapidly. This means that the more we intensify the awareness, the number of individuals with the virus keep decreasing and gradually with time the virus will be wiped out in the population. Similarly, in Figure 4(b), the number of unaware infected increases fast in the quarantined human, but when the number of unaware infected individuals becomes aware of the virus the population decreases. In Figure 4(c), we observed that in the vaccinated humans the impact of education awareness is not pronounced because the population is already aware of the virus and it is vaccinated but it shows a slight increase as a result of the education awareness. Figure 4(d), shows that if the population of recovered humans are aware they will be reduced to susceptible humans. Generally, the impact of public health education campaign can help in reducing the population with the virus when we intensify the campaign awareness.

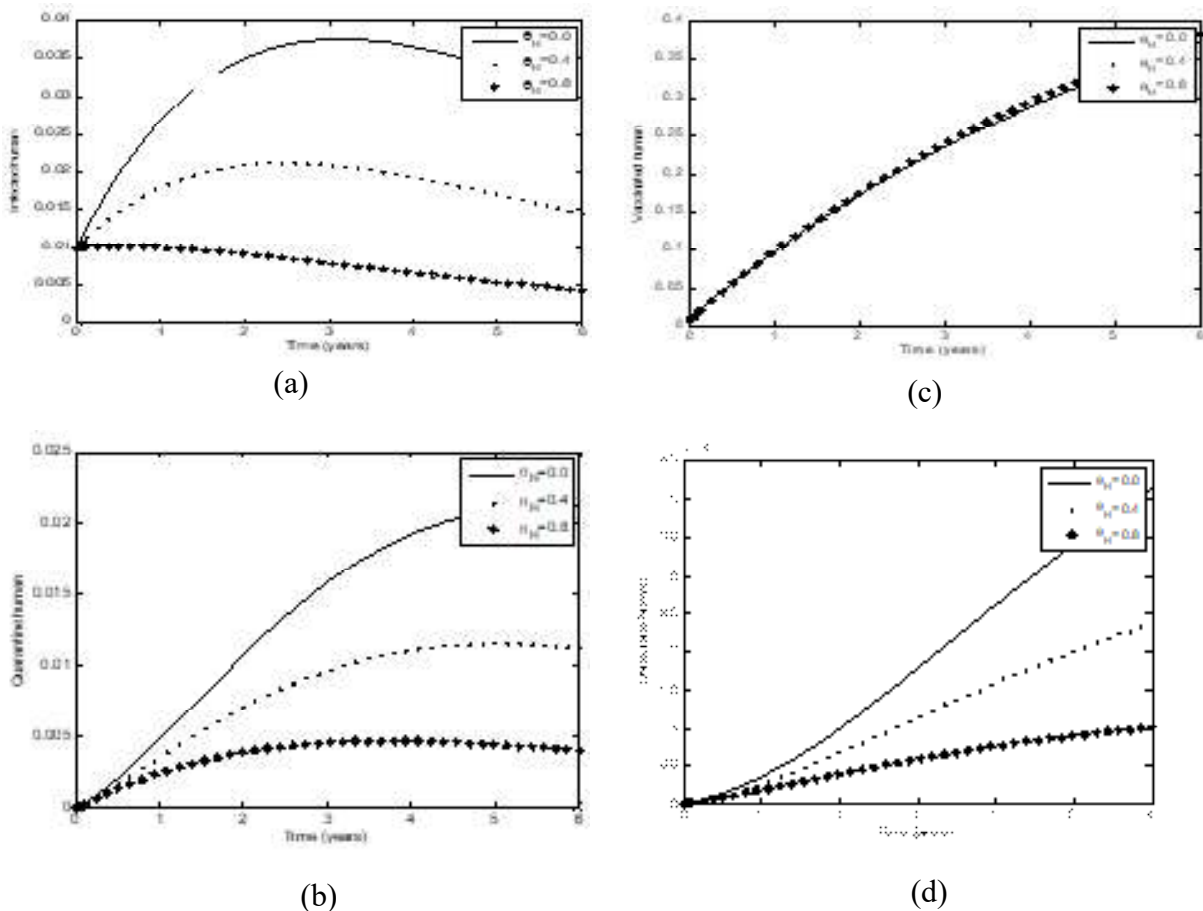
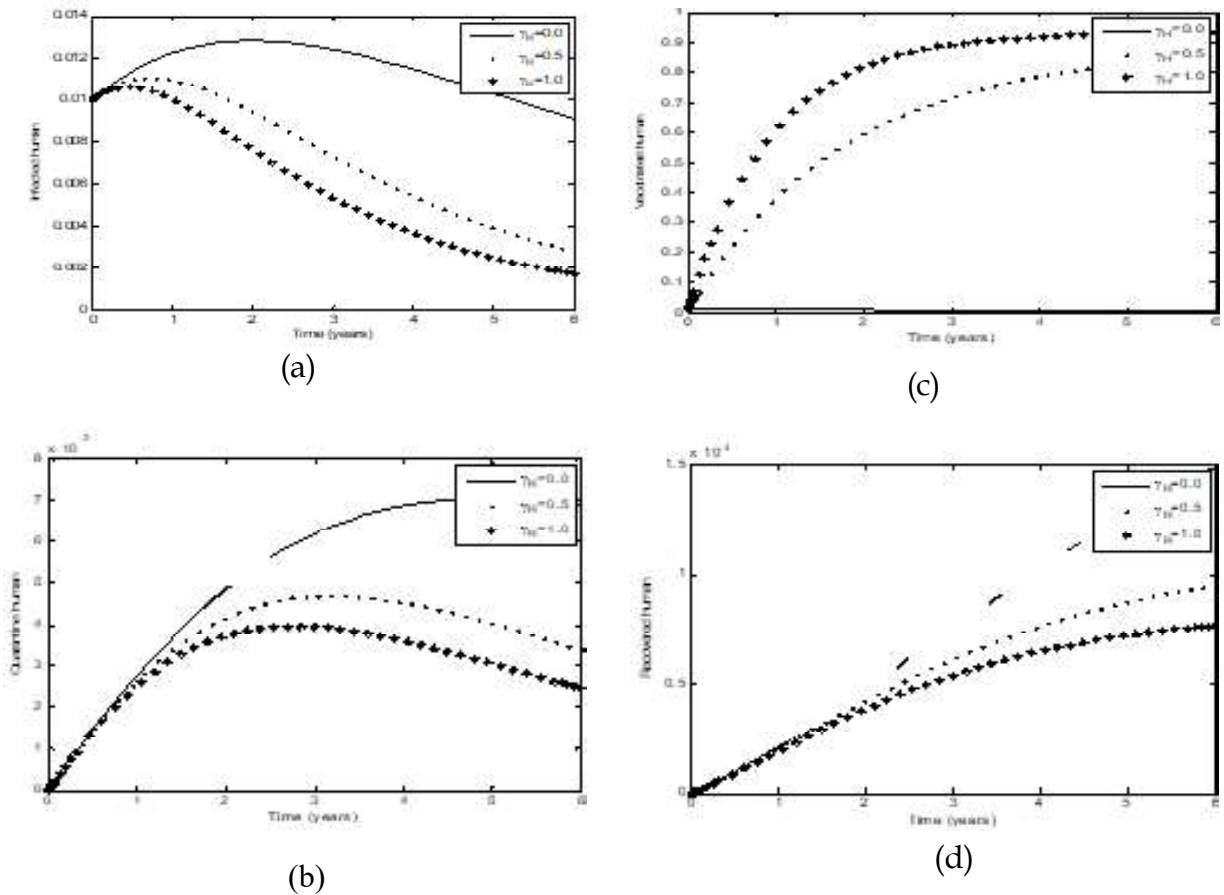


Figure 4: Simulation results showing the effects of public health education campaign ( $\theta_H$ ) on (a) Infected human, (b) Quarantined

human, (c) Vaccinated human and (d) Recovered human.

**Numerical results on the effect of vaccination on the Infected, Quarantined, Vaccination and Recovery**



**Figure 5: The effect of vaccination on the infected, quarantined, vaccination and recovery**

The effect of vaccination on the infected humans increases as shown in Figure 5(a), the effect of vaccination on the infected humans has impact on the population because the vaccine can help protect against certain diseases by imitating an infection. This means that the more we intensify the awareness of the vaccine for the infected population the number of individuals with the virus keep decreasing and gradually with time the virus will be wiped out in the population

In Figure 5(b), the number of those not vaccinated increases fast in the quarantine humans, but when the number of those not vaccinated becomes vaccinated against the virus the population decreases. The more we intensify the vaccination, the more the virus will gradually decrease and be wiped out of the population.

In Figure 5(c), we observed that as we carry out vaccination, the population grows,

that is with time everybody will be vaccinated thus giving no room for individuals to contract the disease.

In Figure 5(d), we observed that the population of the people in the recovered humans, if vaccinated will be reduced to susceptible humans. Generally, the effect of vaccination can help reduce the population with the virus.

**Conclusion**

A deterministic model for the transmission dynamics of avian influenza is developed and analyzed. The model incorporates vaccination and public enlightenment campaign in the human population. The effective reproduction number was computed using the next generation method. The disease-free equilibrium of the model was shown to be locally and globally asymptotically stable when the associated reproduction number is then less unity. Sensitivity analysis was

also carried out and results show that some of the sensitive parameters are the infection transmission rate for birds ( $\beta_A$ ), isolation rate of human with avian strain ( $\beta_H$ ) and public enlightenment campaign ( $\beta_H$ ). Finally, numerical simulation result suggests that vaccination and public enlightenment campaign should be strengthened in the population if avian influenza must be curtailed.

## References

- Abdul, M. and Ashabul, H. (2020). A Mathematical Model of Avian Influenza Poultry Farm and its Stability Analysis. *An International Journal of Application and Applied Mathematics (AAM)*, 15(2): 1091-1113.
- Chairat, M. (2017). Mathematical Modelling of an Avian Influenza: Optimal Control Study for Intervention Strategies. *An International Journal of Applied Mathematics and Information Sciences*, 11(4): 1049-1057.
- Driessche, P. and Watmough, J. (2002). Reproduction Numbers and Sub-thresholds Endemic Equilibrium for Compartmental Models of Disease Transmission. *Mathematical Biosciences*, 180:28-48.
- Kimbir, A. R., Aboiyar, T. and Okolo, P. N. (2014). A Model Formulation for the Transmission Dynamics of Avian Influenza Virus. *IOSR Journal of Mathematics*, 10:29-37
- Kang, T., Zhang, Q., and Rang, L. (2019). A Delay Avian Influenza Model with Avian Slaughter: Stability Analysis and Optimal Control, *Statistical Mechanics and its Applications*, 529: 121-544.
- Kharis, M. and Amidi, A. (2018). Mathematical Modelling of Avian Influenza Epidemic with Bird Vaccination in Constant Population. *Journal of Physics: Conference Series*. 983; 0121116.
- Okosun, K. O. and Yusuf, T. T. (2007). Numerical Simulation of Bird Flu Epidemic. *Research Journal of Applied Science* 2(1): 9-12.
- Mishra, B. K. and Sinha, D. N. (2016). Mathematical Model on Avian Influenza with Quarantine and Vaccination, *Journal of Immunological Techniques in Infectious Disease*. 5:4.
- Mouaouine, A., Boukhouima, A., Hattaf, K and Yousfi, N. (2018). A Fractional order SIR Epidemic Model with Nonlinear Incidence Rate, *Advances in Difference Equations*, 160.
- Xiangjun, L. Bing, X. and Shigui, R. (2020) Mathematical modeling of avian influenza A(H7N9) in China. *Journal of Theoretical Biology*, 50: 567-587.
- Hertz, Y. (2022). Predicting avian influenza virus mutation rates. *PLOS Computational Biology*, 11(1): 21-34.
- Anna, S., Pratama, M. I., Rifandi, M., Sanusi, W. and Side, S. (2020). Stability Analysis and Numerical Simulation of SEIR Model for pandemic COVID-19 spread in Indonesia, *Chaos, Solitons and Fractals*, 139, 110072.
- Rangkuti, Y. M., Landong, A., and Firmansyah. (2022). Sensitivity Analysis of SEIR epidemic model of COVID-19 spread in Indonesia. *Journal of Physics*, 2193/1/012092.
- Ashezua, T. T., Gweryina., R. I. and Kaduna., F. S. (2023). Population dynamics of a mathematical model for Monkeypox. *International Journal of Mathematical Analysis and Modelling*, 6(1), 40-63.
- World Health Organization (WHO). Influenza. [Access 2023 June 14]. Available online: <https://www.who.int/teams/global-influenza-programme/surveillance-and-monitoring/burden-of-disease>
- Centre for Diseases Control (CDC). Avian Influenzas (flu) in humans [Accessed 2022 April 28]. Available online: <https://www.cdc.gov/flu/avianflu> 2022.
- World Health Organization (WHO). Avian weekly update number 907 Influenza. [Retrieved on 21st August, 2023.]. Available online: <https://cdc.who.int/media/docs/default-source/wprodocuments/emergency/surveillance/>

- avian-influenza/ai 20230804.
- Meseko, C., Milani, A., Inuwa, B., et. al. (2023). The Evolution of highly pathogenic avian influenza A (H5) in poultry in Nigeria, 2021-2022. *National library of medicine*, 15(6): 1387. doi:10.3390/v15061387.
- Gumel, A.B., Lubuma, J.M.S., Sharomi, O. and Terefe, Y. A. (2017). Mathematics of a sex-structured model for syphilis transmission dynamics. *Wiley* (special issue paper), doi:10.1002/mma.4734.